Characterising EBV-associated lymphoproliferative diseases and the role of myeloid-derived suppressor cells

Collins, Paul; Fox, Christopher P.; George, Lindsay C.; Pearce, Hayden; Ryan, Gordon Brendan; De Santo, Carmela; Mussai, Francis Jay; Lewis, David; Long, Heather M.; Shannon-Lowe, Claire D.

Document Version
Peer reviewed version

Link to publication on Research at Birmingham portal

Characterising EBV-associated lymphoproliferative diseases and the role of myeloid-derived suppressor cells.

Tracking no: BLD-2020-005611R1

Paul Collins (University of Birmingham, United Kingdom) Christopher Fox (Nottingham University Hospitals,) George Lindsay (Birmingham Children's Hospital, United Kingdom) Hayden Pearce (University of Birmingham, United Kingdom) Gordon Ryan (University of Birmingham, United Kingdom) Carmela De Santo (University of Birmingham, United Kingdom) Francis Mussai (University of Birmingham, United Kingdom) David Lewis (Plymouth Hospitals NHS Trust, United Kingdom) Heather Long (School of Cancer Sciences, University of Birmingham, United Kingdom) Claire Shannon-Lowe (The University of Birmingham, United Kingdom)

Abstract:
Chronic active Epstein Barr virus (CAEBV) typically presents as persistent infectious mononucleosis-like disease and/or haemophagocytic lymphohistocytosis, reflecting ectopic EBV infection and lymphoproliferation of T and/or NK-cells. Clinical behaviour ranges from indolent, stable disease through to rapidly progressive, life-threatening disease. Whilst it is thought the chronicity and/or progression reflect an escape from immune control, very little is known about the phenotype and function of the infected cells versus co-resident non-infected population, nor about the mechanisms that could underpin their evasion of host immune surveillance. To investigate these questions, we developed a multicolour flow cytometry technique combining phenotypic and functional marker staining with *in-situ* hybridisation for the EBER RNAs expressed in every infected cell. This allows the identification, phenotyping and functional comparison of infected (EBER^{POS}) and non-infected (EBER^{NEG}) lymphocyte subset(s) in patients' blood samples ex vivo. We have characterised CAEBV and HLH cases with monoclonal populations of discrete EBV-activated T-cell subsets, in some cases accompanied by EBV-activated NK-cell subsets, with longitudinal data on the infected cells' progression despite standard steroid-based therapy. Given that cytotoxic CD8+ T-cells with relevant EBV antigen specificity were detectable in the blood of the best studied patient, we searched for means whereby host surveillance might be impaired. This revealed a unique feature in almost every CAEBV patient studied: the presence of large numbers of myeloid derived suppressor cells which exhibited robust inhibition of T-cell growth. We suggest that their influence is likely to explain the host's failure to contain EBV-positive T/NK-cell proliferation.

Conflict of interest: No COI declared

COI notes:

Preprint server: No;

Author contributions and disclosures: PJC, LG, HP, GR, CDS, FM, HL and CSL performed experiments; PJC, CPF, HL and CSL conceived the experimental approach; PJC, CPF and CSL wrote the paper; CPF, LG, DL provided clinical input.

Non-author contributions and disclosures: No;

Agreement to Share Publication-Related Data and Data Sharing Statement: emails to the corresponding author

Clinical trial registration information (if any):

Characterising Epstein Barr virus-associated lymphoproliferative diseases and the role of myeloid-derived suppressor cells.

Paul J Collins[1,2], Christopher P Fox[3,6], Lindsay George[4], Hayden Pearce[1,2], Gordon Ryan[1], Carmela DeSanto[1,2], Frances Mussai[1,2], David Lewis[5], Heather Long[1,2], Claire Shannon-Lowe[1,2]*.

[1]Institute for Immunology and Immunotherapy, The University of Birmingham, Vincent Drive, Birmingham B15 2TT, UK.

[2]Cancer Research UK Birmingham Centre, The University of Birmingham, Vincent Drive, Birmingham B15 2TT, UK.

[3]Department of Clinical Haematology, City Campus, Nottingham University Hospitals NHS Trust, Nottingham NG5 1PB, UK.

[4]Birmingham Children's Hospital, Department of Clinical Haematology, Steelhouse Lane, Birmingham B4 6NH, UK.

[5]Plymouth Hospitals NHS Trust, Derriford Hospital, Derriford Road, Crownhill, Plymouth, Devon PL6 8DH, UK.

[6]Divison of Cancer and Stem Cells, School of Medicine, University of Nottingham

Correspondence:

Claire Shannon-Lowe, Institute for Immunology and Immunotherapy, University of Birmingham, Vincent Drive, Birmingham B15 2TT, UK

Phone: (44) 121 41 46425

E-mail: c.shannonlowe@bham.ac.uk

Abstract word count	244
Text word count	4789
Figure count	6
Table count	2
Reference count	28

KEY POINTS

1. Patients with EBV-associated T cells and NK cell lymphoproliferative diseases harbour large expansions of myeloid derived suppressor cells that may play a role in suppressing the antiviral T cell response.

2. EBV infected T cells and NK cells persist in patients in large numbers following treatment.

ABSTRACT

Chronic active Epstein Barr virus (CAEBV) typically presents as persistent infectious mononucleosis-like disease and/or haemophagocytic lymphohistocytosis, reflecting ectopic EBV infection and lymphoproliferation of T and/or NK-cells. Clinical behaviour ranges from indolent, stable disease through to rapidly progressive, life-threatening disease. Whilst it is thought the chronicity and/or progression reflect an escape from immune control, very little is known about the phenotype and function of the infected cells versus co-resident non-infected population, nor about the mechanisms that could underpin their evasion of host immune surveillance.

To investigate these questions, we developed a multicolour flow cytometry technique combining phenotypic and functional marker staining with *in-situ* hybridisation for the EBER RNAs expressed in every infected cell. This allows the identification, phenotyping and functional comparison of infected (EBER^{POS}) and non-infected (EBER^{NEG}) lymphocyte subset(s) in patients' blood samples ex vivo. We have characterised CAEBV and HLH cases with monoclonal populations of discrete EBV-activated T-cell subsets, in some cases accompanied by EBV-activated NK-cell subsets, with longitudinal data on the infected cells' progression despite standard steroid-based therapy. Given that cytotoxic CD8+ T-cells with relevant EBV antigen specificity were detectable in the blood of the best studied patient, we searched for means whereby host surveillance might be impaired. This revealed a unique feature in almost every CAEBV patient studied: the presence of large numbers of myeloid derived suppressor cells which exhibited robust inhibition of T-cell growth. We suggest that their influence is likely to explain the host's failure to contain EBV-positive T/NK-cell proliferation.

INTRODUCTION

Epstein-Barr virus is <mark>initially thought to infect</mark> oropharyngeal epithelium before colonising the B-cell system, initially as a growth-transforming infection with expression of the full set of latent cycle genes, followed by transition to an antigenically-silent latency within memory B-cells. Primary infection usually occurs during childhood and is almost always asymptomatic. Delay in primary infection until young adulthood can result in infectious mononucleosis (IM), an acute but self-resolving illness whose febrile symptoms appear to be a product of the host's exaggerated cellular immune response. That response is initiated by natural killer cells (NK), followed by robust CD4+ and particularly CD8+ T-cell responses to lytic and latent cycle viral antigens [1,2]. However, when T-cell function is impaired, for example transplant recipients on immunosuppressive drugs, failure to control latent growth-transforming infection can lead to post-transplant B lymphoproliferative disease [3].

By contrast, primary infection in a rare minority of individuals leads to a chronic, non-resolving condition termed chronic active EBV (CAEBV) encompassing many of the clinical features of IM such as fever, splenomegaly, hepatitis and lymphadenopathy. In CAEBV, however, these symptoms are severe and persist for at least 3 months accompanied by very high EBV DNA load in the blood and extensive organ infiltration by EBV-infected cells. CAEBV can develop into a spectrum of clinical conditions. Patients with indolent disease can remain stable over many years, whilst others display a more rapidly progressive disease with serious complications including haemophagocytic lymphohistiocytosis (HLH), hepatic failure and gastrointestinal ulceration/perforation.

In Western countries, CAEBV is thought to be predominantly associated with EBV infection of B-cells. Previously reported cases of B-cell CAEBV identified defective cytotoxic T lymphocytes (CTLs) [4] or NK-cells [5], in some cases linked to inactivating mutations in the perforin [6] or GATA2 gene [7]; such impairment could explain the chronic nature of the disease. In contrast, CAEBV in South East Asia, Central and South America is predominantly associated with EBV infection of T-cells and NK-cells. In these patients, the clinical features, natural history and prognosis are associated with the phenotypic identity of the infected lineage; patients with T-cell CAEBV exhibit more aggressive disease and significantly inferior survival, while patients with NK-cell CAEBV more often have milder symptoms and a more favourable clinical outcome [8,9]. However, NK-cell CAEBV seems to have a greater propensity (23.1%) for transformation into aggressive NK-cell leukaemia or extranodal NK/T-cell lymphoma [8-10]. Thus the morbidity and mortality conferred by this clinically heterogeneous spectrum of EBV-associated lymphoproliferations is substantial. The high mortality is likely attributable to the paucity of effective treatment options. Immunomodulatory agents are largely ineffective and, while corticosteroids and other immunosuppressive agents temporarily

ameliorate clinical symptoms, patients usually succumb to progressive disease. Currently, allogeneic stem cell transplantation is the only established curative treatment [11-13].

The pathogenesis of T/NK CAEBV is poorly understood. In contrast to B-cell CAEBV, patients with T/NK-cell CAEBV are not thought to have a pre-existing immune defect [10] yet infected cells persist in blood and tissues long-term. These EBV-infected T/NK-cells exhibit a Latency I/II viral gene expression profile (non-coding EBER RNAs, EBNA1 +/- LMP1 and LMP2a/TR) [14] and should therefore elicit a T-cell response. This suggests that T-cell responses are either absent or in some way functionally inhibited. This hypothesis is supported by clinical experience in this context, whereby infusions of third-party EBV-specific CTLs have proven ineffective against progressive disease [15]; suggesting an inhibitory mechanism is at play.

To address the many issues raised by the different presentations of CAEBV and EBV-associated LPDs, we developed a protocol, applicable to blood cell preparations ex-vivo, to inform patient management while helping to understand disease pathogenesis. Here we describe a protocol that combines EBER in-situ hybridisation, allowing visualisation and enumeration of EBV-infected cells, with cell surface and intracellular staining for a whole range of phenotypic and functional markers relevant to B, T or NK-cells and their subsets. This protocol was applied to five UK patients, all initially diagnosed as CAEBV or as HLH which were found to be EBV-related. Two proved to have B-cell infection; three had monoclonal T-cell or NK-cell infections whose progression could be followed despite attempts at therapy. Surprisingly this same study revealed another unexpected but consistent feature of blood samples from T/NK CAEBV patients, the presence of large numbers of circulating myeloid-derived suppressor cells (MDSCs) with the ability to suppress T-cell responses in in-vitro assays. This points to a potential link between MDSC-mediated T-cell inhibition and the chronic progressive nature of CAEBV.

METHODS

Ethical approval

This research received institutional approval from the University of Birmingham and studies of clinical material received ethical approval from the South Birmingham NRES Committee (07/H1208/62). All patients and healthy volunteers provided written informed consent in accordance with the Declaration of Helsinki.

Flow cytometry

PBMCs (5×10^6 cells) were stained using Fixable Viability Dye eFluor-450 or eFluor-780 (ThermoFisher) for 30 min at 4°C. Cell surface staining was then performed with fluorophore-conjugated antibodies (Table 1) for 30 min at 4°C. MDSCs were pre-incubated with purified human IgG (5 μg/ml) for 15 min at 4 °C prior to addition of mAbs. For intracellular staining, cells were fixed and permeabilised using the TrueNuclear™ Transcription Factor buffer Set (Biolegend) according to the manufacturer's instructions then labelled with antibodies (Table-1) for 30 min at room temperature. Fluorescence data was acquired using a LSR II or LSRFortessa X-20 (Becton Dickinson; BD) and analysed in FlowJo software version 7.6.5 (Tree Star).

FlowRNA for detection of EBV-encoded RNAs (EBERs)

FlowRNA experiments were performed on $1\text{-}3 \times 10^6$ PBMC (PrimeFlow RNA, Thermo Fisher), according to the manufacturer instructions. A full description of the protocol can be found in supplementary information. Briefly, cells were stained using Fixable Viability Dye eFluor™-450, then for cell surface markers (Table 1). Cells were fixed, permeabilised and intracellular staining performed in the presence of RNase inhibitors. Cells were fixed again then target RNA was hybridised using Target Probe sets (custom designed by PrimeFlow RNA, Thermo Fisher) for (i) EBER-1/2 and (ii) β2-microglobulin (B2M). Briefly, the probes were hybridised at 40°C for 3 hours, washed then subjected to sequential hybridization at 40°C using the 'PreAmplifier', 'Amplifier' and fluorescent label (Type-1 probes, AlexaFluor®-647; Type-2 probes, AlexaFluor®-488). Cells were acquired using a LSRII or LSRFortessa X-20 and analysed in FlowJo software version 10.

Measurement of cytokines in plasma

Plasma was collected following density centrifugation (Lymphoprep, Stemcell Technologies) of fresh EDTA blood samples. Plasma was immediately snap-frozen in liquid nitrogen and stored at -80°C until use. Cytokines in plasma (IL-1β, IL-4, IL-6, IL-10, IL-17A, IFNγ, GM-CSF, TNFα) were measured using a custom ProcartaPlex™ bead-based immunoassay (ThermoFisher) according to manufacturer's instructions. Arginase-1 in plasma was measured by ProcartaPlex™ Singleplex immunoassay. Mean fluorescence intensity of each analyte was detected using a Luminex 200 instrument (R&D Systems, UK).

T lymphocyte proliferation assay

Positive magnetic assisted cell sorting (MACS) using anti-human CD15 microbeads and MACS LS separation columns (Miltenyi Biotech) were used to isolate CD15+ G-MDSC from the PBMC. T lymphocytes were obtained from the PBMC by negative selection following removal of CD15+ cells. T-cells ($2x10^5$/well) were cultured in 96-well flat-bottom plates coated with anti-CD3 (OKT3; 3µg/ml) and anti-CD28 (2µg/ml) (eBioscience), in 200µl complete medium supplemented with 0.1% β-mercaptoethanol (ThermoFisher). Cells were incubated for 4 days at 37 °C, 5% CO_2 and proliferation determined by ^{3}H-thymidine (Perkin Elmer Life Sciences) incorporation using a TopCount NXT scintillation counter (Perkin Elmer). MDSC-mediated suppression was determined by co-culture with T-cells. Results are expressed as a percentage of T-cell proliferation driven by CD3/28 ligation in the presence of MDSCs, relative to T-cell proliferation in their absence (100%).

H&E staining of blood smears and PBMC cytospins

Fresh blood was smeared on glass slides and freshly-isolated PBMC were spun onto glass slides, air-dried then fixed in 100% methanol for 1 minute.

Statistical analysis

Statistical tests used are indicated in relevant sections. All experiments where tests have been applied were performed on at least 3 donors. Tests were considered statistically significant if $p < 0.05$.

RESULTS.

Set-up and Validation of Multicolour FlowRNA.

To identify the lymphocyte subset infected by EBV we established a multicolour flow cytometry-based assay (FlowRNA) to simultaneously detect the abundantly expressed viral non-coding RNAs (EBER-1/2), present in every infected cell, together with lymphocyte subset markers CD3, CD4, CD8, CD19 and CD56 on $1\text{-}2 \times 10^6$ fresh mononuclear leukocytes (PBMC). The assay (Figure 1a), involved cell surface staining, cell fixation, permeabilization, intracellular staining then in-situ hybridisation (ISH) for the viral EBERs, and for Beta-2-microglobulin (B2M) transcripts as a positive control. The cells were analysed by flow cytometry; lymphocytes were identified by Forward vs Side Scatter and CD14+ monocytes, dead cells and cell doublets were excluded from all subsequent analysis (Figure 1b). The assay was initially validated by adding decreasing numbers of EBV+/GFP+ Akata cells to EBV-/GFP- Akata cells. The dual EBER+/GFP+ populations matched the input cell number and demonstrated assay sensitivity and specificity (Figure 1c). EBV-infected lymphocyte subsets were not identified in the blood of healthy EBV carriers (n=10), where the percentage of infected B-cells was below the threshold of detection (Figure 1d). However, the assay unambiguously identified EBV-infected subsets in previously frozen reference samples from patients with EBV-associated LPDs. In the case shown, EBV was detected in CD3+/CD8+ T-cells with a small fraction detected in CD19+ B-cells (Figure 1d). In terms of virus load detectable by FlowRNA, provided at least 500×10^5 total patient lymphocytes were analysed by flow cytometry, we found the lowest viral load detected by the FlowRNA assay was approximately 8×10^4 virus copies/ml blood.

Identification of EBV-infected lymphocytes by Multicolour FlowRNA.

The clinical data for all five patients is summarised in Table 2 and expanded upon in Supplementary Data. Each patient presenting with EBV-associated LPDs had high EBV loads measured in whole blood, enabling the identification and enumeration of infected lymphocyte subsets directly from blood. The FlowRNA revealed clear populations of EBER-positive (EBER^POS) and EBER-negative (EBER^NEG) lymphocytes; no other cell types, including myeloid cells, were EBER^POS. In patients 1 and 2, the EBER^POS cells were identified as CD19+ B-cells (Figure 2a), where approximately 1% of total B-cells were EBER^POS. Whilst this appears to be relatively low, detection of EBV in 1% of B-cells is remarkably high, equivalent to the number of EBV-infected B-cells in the blood of acute IM patients [16]. In contrast, the numbers of EBV-

infected B-cells in healthy carriers is on average one B-cell in 10,000 [17], below the threshold of detection of the assay (Figure 1d).

In patients 3 and 4, FlowRNA revealed EBV infection of the CD4+ T-cells (Figure 2b). The percentage of EBER[POS] cells within the total CD4+ T-cell population was high for both patients; 49% from patient 3 and 40% from patient 4. Patient 5 had a more complex profile of non-B-cell infection. EBV was detected in at least 80% of total CD56+ NK-cells, 100% of which were CD56^{high} (Figure 2b). EBV was also detected in CD4+, CD8+ T-cells, and CD19+ B-cells.

Notably, the level of CD3 expression was down-regulated on the EBER[POS] T-cells but not the EBER[NEG] T-cells, shown by mean fluorescence intensity (MFI) in Figure 2b. The MFI of CD3 expression was slightly but consistently lower on the EBER[POS] T cells from patient 3 and 5 compared to the EBER[NEG] T cells; (patient 3 CD4+ T-cells CD3 MFI: EBER[POS] 446 vs EBER[NEG] 614; patient 5 CD4+ T-cells CD3 MFI: EBER[POS] 1240 vs EBER[NEG] 2019 and CD8+ T-cells CD3 MFI: EBER[POS] 459 vs EBER[NEG] 1204). However, the MFI of CD3 expression on the EBER[POS] CD4+ T-cells from patient 4 was significantly lower than the CD3 expression on the EBER[NEG] cells (MFI: EBER[POS] 210 vs EBER[NEG] 1054).

Clonality of the EBV-infected T-cells

The EBV-associated T/NK-cell LPDs are considered monoclonal/oligoclonal proliferations of EBV-infected T/NK-cells due to the presence of a monoclonal virus [18]. To extend these findings, we investigated T-cell receptor (TCR) clonality of the EBER[POS] vs the EBER[NEG] CD4+ T-cells using a panel of mAbs directed against Vβ epitopes to delineate the TCRαβ repertoire. The TCR-BV usage in the EBER[POS] CD4+ T-cells from patients 3 and 4, and the EBER[POS] CD8+ T-cells from patient 5 revealed the presence of a monoclonal EBV proliferation; TCR-BV8, TCR-BV12 and TCR-BV13.2 respectively (Figure 2c). However the EBER[POS] CD4+ T-cells from patient 5 were a clonally-diverse EBV-positive T-cell population. In contrast, the total EBER[NEG] CD4+ and CD8+ T-cells from each patient retained a heterogeneous spread of TCR-BV usage (Figure 2c). Single cell cloning of the EBER[POS] and EBER[NEG] CD4+ T-cells from patient 4 and subsequent sequencing of the TCR Vα and Vβ chains confirmed the TCR-BV8 had identical CDR3 DNA sequences (Supplementary Data).

Phenotype and Function of EBV-infected CD4+ T-cells

The adaptability of FlowRNA enabled the simultaneous comparison of phenotype and function between EBER[POS] and EBER[NEG] cells directly from patient blood, with matched lymphocyte subsets from healthy controls (n=6). We developed FlowRNA panels to examine markers of

T-cell subsets, activation, proliferative status and functional capacity to determine how EBV alters the phenotype and function of infected cells. We added CD45RA and CCR7 to discriminate between naïve (N: CD45RA+, CCR7+), central memory (CM: CD45RA-, CCR7+), effector memory (EM: CD45RA-, CCR7-) and terminally differentiated effector (TEMRA: CD45RA+, CCR7-) CD4+ T-cells; CD38 and Ki67 to examine activation and proliferative status; Foxp3 and CD25 to identify regulatory T-cells (Treg); plus IFNγ and TNFα to examine functional capacity.

Interestingly, EBV infection appeared to be confined to memory T cells. The EBER[POS] CD4+ T-cells from patients 3 and 4 expressed neither CD45RA nor CCR7, consistent with memory (Figure 3, top row). In contrast, the EBER[NEG] CD4+ T-cell population maintained N, CM, EM and TEMRA CD4+ T-cell subsets at similar ratios to those observed in healthy donors; 2 representative donors shown (Figure 3a). These EBER[POS] CD4+ T-cells also showed greater levels of activation and proliferation (CD38 and Ki67) than the EBER[NEG] CD4+ and healthy donor CD4+ T-cells. In patient 3, over 60% of EBER[POS] cells expressed CD38, with at least 15% of these co-expressing Ki67. In patient 4, the majority of EBER[POS] cells expressed high levels of CD38 and co-expressed Ki67 (Figure 3b). Such findings suggest that EBV may be driving the activation and proliferation of infected cells.

Examination of markers of Tregs, FoxP3 and CD25, revealed the EBER[POS] cells were not Tregs. Furthermore, there was no evidence of increased numbers of Tregs in the EBER[NEG] population, compared to healthy donors (range 3 – 4%) (Figure 3c). However, EBV appeared to significantly alter the cytokine expression profile of infected cells in patients 3 and 4. Patient and healthy donor PBMCs were stimulated for 6 hours with PMA and ionomycin in the presence of brefeldin A, followed by intracellular cytokine staining. EBER[POS] CD4+ T-cells exhibited remarkably different cytokine expression profiles. Whilst the majority (>70%) of EBER[POS] cells from patient 3 produced IL-17A and IFNγ, the majority (>80%) of EBER[POS] cells from patient 4 produced TNFα and/or IFNγ (Figure-3d) but little IL-4 and IL-17 (data not shown). In comparison, the EBER[NEG] CD4+ T-cells from both patients exhibited a cytokine expression profile broadly similar to that of healthy donor CD4+ T-cells (Figure 3d), with low abundance of IL-4 and IL-17A expressing cells (data not shown).

To investigate whether the EBV infected CD4+ T cell clones were EBV specific, we tested their capacity to produce IFNγ in response to stimulation with a panel of HLA II-matched LCLs. In these preliminary analyses, no response was seen (data not shown), however further studies are required to determine the specificity of the EBV-infected CD4+ T cells.

EBV-infected T-cells are refractory to treatment

We received blood from patient 3 following a diagnosis of HLH; the peripheral blood EBV load was 673,035 EBV DNA copies/ml and the EBER[POS] cells accounted for 17% of their total CD4+ T-cells (Figure 4a). The patient was treated with corticosteroids and etoposide for the next 6 weeks, based on the HLH-2004 protocol [19]. After this initial phase of therapy (8 weeks post-treatment), although the clinical and laboratory features of HLH had resolved, EBV load was consistently above 10^6 copies/ml and the proportion of EBER[POS] CD4+ T-cells had increased more than 4-fold to 72% (Figure 4a). The total WBC counts and lymphocyte counts for the initial pre-treatment and post treatment samples were within the normal ranges and the counts were very similar (**WBC**: 4.1 cells/μl vs 8.0 cells/μl for pre- vs post-treatment; **lymphocytes**: 1.7 cells/μl vs 1.6 cells/μl for pre- vs post-treatment). The patient subsequently underwent an Alemtuzumab-based, reduced-intensity conditioned HSCT from a matched unrelated donor. Prior to transplant, the proportion of CD4+ T-cells infected with EBV remained high, at around 50%. Immediately following HSCT, EBV became undetectable in peripheral blood and remained so for >18 months post-transplant, aside from one episode of low-level reactivation where we confirmed the virus was exclusively in the B-cells; successfully treated with rituximab. However, the patient's EBV DNA load began to rise rapidly at 21 months post-transplant (from 34,950 to 684,750 copies/ml over a 3 week period). At 22 months post-transplant, we confirmed re-emergence of EBV-infected CD4+ T-cells in the peripheral blood (Figure 4b). The patient died approximately 6 weeks after this date. The CD4+ T-cell population comprised 40% of cells positive for TCR-BV8 (Figure 4c), suggesting that the original clone of EBV-infected CD4+ T-cells had persisted following transplantation and subsequently recrudesced, leading to disease relapse.

Patient 4 initially presented with reactive lymphadenopathy, gastritis with benign histological appearances and high EBV load. After 6 months a gastric biopsy demonstrated a dense infiltration of mature T-cells, predominantly EBV+ CD4+ and an EBV load of 1,393,353 EBV DNA copies/ml. We received our initial sample at this point where EBER[POS] cells accounted for 16% of their total CD4+ T-cells. He received steroid treatment followed by GDP (gemcitabine, dexamethasone, cisplatin) chemotherapy with some initial clinical improvement. Subsequent EBV load showed a climb to >8,000,000 EBV DNA copies/ml and the proportion of EBER[POS] CD4+ T-cells increased 2.5-fold to 40% (Figure 4a). He was planned for SMILE (dexamethasone, methotrexate, ifosfamide, asparaginase, etoposide) chemotherapy but became acutely unwell and died due to bowel ischaemia.

Phenotype and Function of EBV-infected CD4+, CD8+ T+ and NK-cells from ANKL.

At initial presentation with HLH, the vast majority of EBER[POS] cells were CD56^{high} NK-cells, with small additional populations of EBER[POS] CD4+ and CD8+ T-cells. We therefore examined the phenotype and function of all infected subsets and their EBER[NEG] counterparts. As observed in patients 3 and 4, EBV infection of the CD4+ and CD8+ T-cells from patient 5 was restricted to cells without CD45RA and CCR7 expression, consistent with a memory phenotype (Figure 5a and 5e); the EBER[NEG] T-cells and matched healthy controls maintained the expected distribution of naïve and memory CD4+ T-cell populations. However the EBER[POS] CD4+ T-cells completely lacked expression of the activation/proliferation markers CD38 and Ki67, with expression matching that of the EBER[NEG] CD4+ T-cells and matched healthy controls, suggesting EBV had not activated these infected cells. Furthermore, the EBER[POS] CD8+ T-cells exhibited low levels of activation but little evidence of proliferation (Figure 5b and 5f).

The EBER[POS] CD4+ were not Tregs (CD25-, FoxP3-), and the proportion of Tregs within the EBER[NEG] or healthy control populations was not increased (Figure 5c and 5g). However, the majority of EBER[POS] CD4+ T-cells expressed TNFα (+/- IFNγ) with only a subset expressing neither cytokine (Figure 5d and 5h). All the EBER[POS] CD8+ T-cells expressed IFNγ and TNFα, or IFNγ alone. In comparison, over half the EBER[NEG] CD8+ T-cells expressed neither cytokine.

Finally, we examined the same markers on the NK-cells. The EBER[POS]CD56^{high} NK-cells lacked expression of CD45RA and CCR7 (Figure 5i), unlike the EBER[NEG] patient and healthy donor NK-cells which expressed CD45RA alone. The entire populations of EBER[POS] and EBER[NEG] NK-cells were activated (CD38+), although only the EBER[POS] cells co-expressed Ki67 (Figure 5j), and the majority of EBER[POS] and EBER[NEG] NK-cells expressed either TNFα alone or in combination with IFNγ. In contrast, nearly 50% of healthy donor NK-cells expressed neither cytokine (Figure 5k). Initial examination of the CD56^{high} NK cells revealed low level expression of CD16, however further analysis was precluded due to the rapid death of the patient.

Myeloid-derived suppressor cells are expanded in the blood of patients, and potently inhibit T-cell responses.

Analysis of fresh patient blood revealed large expansions of cells resembling neutrophils that co-purified with PBMCs following density centrifugation. Such cells were present at low abundance in healthy donor blood (n=6, <0.5% of PBMC) but outnumbered lymphocytes in

three of the five cases (Figure 6a and 6b). These cells had nuclear morphology typical of cells undergoing granulopoiesis (Figure 6c) and expressed CD11b+, CD15+, CD16+ CD33+ but CD14- and HLA class II- (Figure 6d), confirming their identity as myeloid-derived suppressor cells of granulocyte lineage (G-MDSCs).

Numerous growth factors and cytokines are thought to drive the expansion and suppressive activity of MDSCs. Luminex assays performed on patient plasma revealed the presence of high concentrations of GM-CSF, IL-1β, IL-6 and TNFα (Figure 6e) as well as IL-4, IFNγ and IL-10 (data not shown) relative to healthy individuals. Additional analysis of plasma from a banked collection of EBV-associated HLH patients (details provided in Supplementary material) also showed increased concentrations of these same cytokines. Furthermore, analysis of tissue culture medium from EBV-infected T cell clones established from CAEBV patients, but not the EBV uninfected T cell clones, also contained high concentrations of these cytokines (data not shown), suggesting the EBV-infected cells themselves are producing the cytokines observed in the patient plasma. Interestingly, we cloned EBV-specific CTLs from one patient that showed recognition of LMP1 epitopes, exhibited epitope-specific degranulation and ability to kill autologous cells presenting these epitopes (Supplementary Figure 1).

MDSCs are thought to suppress effector T-cell growth and function through a number of mechanisms, including production of arginase-1. T-cells depend on L-arginine for proliferation and function are particularly sensitive to arginine-depletion by arginase-1. Luminex analysis showed an increase in the concentration of arginase-1 in patient plasma compared to healthy donors, where the concentration was below the level of detection (Figure 6f).

MDSCs are highly labile and cryosensitive, therefore functional studies were performed on freshly-isolated patient MDSCs. *Ex vivo* MDSCs were co-cultured with allogeneic T-cells pre-labelled with tritiated thymidine to analyse the growth of the T-cells in the presence of MDSCs. T-cell growth was increasingly suppressed when co-cultured with increasing MDSCs at T-cell: MDSC ratios from 1:0.125 up to 1:1, compared to T-cells cultured alone (Figure 6g). Furthermore, T-cells co-cultured with MDSCs at a 1:1 ratio exhibited significant growth inhibition when compared to culture with MDSCs from healthy individuals (p=0.0377) and to T-cell growth alone (p=0.0206) (Figure 6h).

DISCUSSION

FlowRNA has significant clinical utility. The assay is particularly useful in confirming the differential diagnosis of an EBV-associated B-cell vs T/NK-cell LPD. This timely confirmation is important when considering targeted treatment options, monitoring treatment outcomes and identifying early relapse. This potential was clearly demonstrated for one patient who received HSCT due to EBV-infected CD4+ T-cells. Following HSCT, FlowRNA identified an expansion of EBV-infected B-cells, which was successfully treated with rituximab. The FlowRNA subsequently detected disease relapse arising from a re-emergence of the original EBER[POS] CD4+ T-cell clone.

FlowRNA has provided fundamental insights into disease pathogenesis. Although we and others have previously reported infection of more than one lymphocyte subset in patients with T/NK-cell LPDs [10,20], it is not currently known if all infected subsets contribute to the disease. Our data suggests perhaps not. When comparing the activation status of the EBER[POS] CD4+ T-cells from patients 3, 4 and 5, the CD4+ T-cells from patient 5 showed a lack of activation, no difference in cytokine expression between the EBER[POS], EBER[NEG] and healthy donor CD4+ T-cells, and lack of clonality. In the context of multiple subset infection, these EBER[POS] CD4+ T-cells may be bystander infections that contribute little to the overall disease pathogenesis and may represent early infection of progenitor cells before TCR rearrangement.

Decreases in CD3 and TCR expression were revealed on all EBER[POS] T-cells relative to their uninfected counterparts. As exemplified in patient 4, high level of activation is known to decrease cell-surface levels of CD3 and TCR, and indeed these cells co-expressed high levels of activation markers, CD38 and Ki67. Interestingly, EBV infection appears to be restricted to CD45RA-/CCR7- memory T-cells. This is reminiscent of B-cell infection where EBV drives germinal centre-independent mutagenesis and clonal evolution of immunoglobulin genes in naïve B-cells to make them resemble memory B-cells [21]. Perhaps EBV also drives TCR-independent differentiation from naïve to memory T-cells.

Whilst the clonal EBER[POS] CD4+ T-cells were consistent in their differentiation and activation status, their cytokine expression profile differed. Although we expected these differences would co-segregate with clinical presentation, this was actually not the case. Instead, the infected CD4+ T-cells exhibited differing cytokine expression profiles, irrespective of the disease. This suggests that EBV infection does not inhibit the functional differentiation of CD4+ T-cells. Interestingly, the uninfected CD4+ T-cells from patients and healthy donors were remarkably similar in phenotype and function, suggesting the uninfected cells were unaffected by the chronic inflammatory microenvironment.

Understanding how EBV-infected T- and NK-cells evade immune surveillance is of fundamental importance, particularly in the context of limited effective therapeutic options. MDSCs play a pivotal role in suppressing host immunity. Although most intensively studied in cancer, MDSCs are also generated as a result of chronic viral infection (including HCV, HIV and HBV), where they modulate the immunopathology and inhibit the antiviral T cell response [22-24]. Although the evidence presented in this report demonstrates *in vitro* inhibition of T cell growth by the patient's MDSCs, it does suggests that the MDSCs may be performing a similar role to that observed in the previously reported chronic infection scenarios. Thus, the MDSCs may be suppressing the antiviral T-cell response and enabling the persistence of the EBV-infected cells in the EBV-associated T cell and NK cell LPDs, although further investigation is required. In addition, previous reports of chronic infections have also demonstrated the virally infected cells secrete factors that drive the activation and expansion of MDSCs. This may be achieved, at least in part, by their expression of growth factors (GM-CSF, G-CSF) and pro-inflammatory cytokines (IL-1β, IL-6, TNF-α) [25,26]. These growth factors and pro-inflammatory cytokines are often highly induced in chronic infection and stimulate the activation of myeloid progenitors, but may also drive the expansion and activation of MDSCs [27,28]. Furthermore, the mechanisms of MDSC-mediated inhibition of T cell growth and function are known to include arginase-1, reactive oxygen (ROS) and nitrogen (NOS) species. These mechanisms can be blocked by inhibitors, resulting in the expansion of T cells in the presence of MDSCs. Although we were unable to perform these experiments *ex vivo* due to the lack of patient samples, given the raised concentrations of Arginase-1 in the patient plasma, it is highly likely these mechanisms play at least some role in the inhibition of T cell growth and function in these patients.

A major finding of this study is that the EBV-infected T/NK-cells appeared to be refractory to treatment with the HLH2004 regimen containing etoposide, dexamethasone and cyclosporin A. For our evaluable patients, the number of EBV-infected cells increased in number whilst the total WBC and lymphocyte counts remained within the normal range and both the pre- and post-treatment samples were very similar in number. The large expansion of infected cells following treatment suggests that a subset of infected cells were resistant to the DNA damaging agent etoposide and were able to rapidly grow following the end of treatment. However, further studies are required to determine if the infected cells expanded throughout the course of treatment or indeed after treatment stopped. Corticosteroid treatment, usually dexamethasone or methylprednisolone, is a central component of commonly used protocols for EBV-associated HLH and CAEBV. The rationale for steroid-containing regimens is suppression of the transcription of T-cell effector cytokines. However, an important consequence is the loss of the effector T-cells from the circulation. These effector T-cells

may play a role in controlling the outgrowth of the EBV-infected cells and their loss may contribute to the expansion of infected cells following treatment. Therefore, one of two mechanisms could be restricting the outgrowth of the EBV-infected T/NK-cells; the MDSCs themselves or residual activity of endogenous EBV-specific CTLs. In either scenario, corticosteroids would disrupt this restriction, leading to unchecked expansion of infected T/NK-cells.

Although only demonstrated in a small number of patients, these data appear to have major implications for therapy. The FlowRNA assay will therefore enable a thorough examination of how the number and function of EBV-infected T/NK cells impact on disease outcome and relapse following therapy and provide a better understanding of the implications of using agents such as etoposide and corticosteroids as first-line therapy. Secondly, the presence of MDSCs in other chronic viral infections have a significant impact on the disease outcome, particularly when considering the use of cell-based therapies. A thorough understanding of the role of MDSCs in EBV-associated HLH and CAEBV will enable a more targeted approach to treat these patients without the need for resorting to stem cell transplants.

ACKNOWLEDGMENTS

AUTHORSHIP CONTRIBUTIONS

PJC, LG, HP, GR, CDS, FM, HL and CSL performed experiments; PJC, CPF, HL and CSL conceived the experimental approach; PJC, CPF and CSL wrote the paper; CPF, LG, DL provided clinical input.

DISCLOSURE OF CONFLICT OF INTEREST

The authors declare no conflict of interest.

REFERENCES

1.   Long HM, Meckiff BJ, Taylor GS. The T-cell Response to Epstein-Barr Virus-New Tricks From an Old Dog. *Front Immunol*. 2019;10:2193.

2.   Munz C. Epstein-Barr Virus-Specific Immune Control by Innate Lymphocytes. *Front Immunol*. 2017;8:1658.

3.   Shannon-Lowe C, Rickinson A. The Global Landscape of EBV-Associated Tumors. *Front Oncol*. 2019;9:713.

4.   Fujieda M, Wakiguchi H, Hisakawa H, Kubota H, Kurashige T. Defective activity of Epstein-Barr virus (EBV) specific cytotoxic T lymphocytes in children with chronic active EBV infection and in their parents. *Acta Paediatr Jpn*. 1993;35(5):394-399.

5.   Joncas J, Monczak Y, Ghibu F, et al. Brief report: killer cell defect and persistent immunological abnormalities in two patients with chronic active Epstein-Barr virus infection. *J Med Virol*. 1989;28(2):110-117.

6.   Katano H, Ali MA, Patera AC, et al. Chronic active Epstein-Barr virus infection associated with mutations in perforin that impair its maturation. *Blood*. 2004;103(4):1244-1252.

7.   Cohen JI. GATA2 Deficiency and Epstein-Barr Virus Disease. *Front Immunol*. 2017;8:1869.

8.   Kimura H, Hoshino Y, Hara S, et al. Differences between T cell-type and natural killer cell-type chronic active Epstein-Barr virus infection. *J Infect Dis*. 2005;191(4):531-539.

9.   Kimura H, Morishima T, Kanegane H, et al. Prognostic factors for chronic active Epstein-Barr virus infection. *J Infect Dis*. 2003;187(4):527-533.

10.   Okuno Y, Murata T, Sato Y, et al. Defective Epstein-Barr virus in chronic active infection and haematological malignancy. *Nat Microbiol*. 2019;4(3):404-413.

11.   Gotoh K, Ito Y, Shibata-Watanabe Y, et al. Clinical and virological characteristics of 15 patients with chronic active Epstein-Barr virus infection treated with hematopoietic stem cell transplantation. *Clin Infect Dis*. 2008;46(10):1525-1534.

12.   Kawa K, Sawada A, Sato M, et al. Excellent outcome of allogeneic hematopoietic SCT with reduced-intensity conditioning for the treatment of chronic active EBV infection. *Bone Marrow Transplant*. 2011;46(1):77-83.

13.   Sawada A, Inoue M, Kawa K. How we treat chronic active Epstein-Barr virus infection. *Int J Hematol*. 2017;105(4):406-418.

14.   Fox CP, Haigh TA, Taylor GS, et al. A novel latent membrane 2 transcript expressed in Epstein-Barr virus-positive NK- and T-cell lymphoproliferative disease encodes a target for cellular immunotherapy. *Blood*. 2010;116(19):3695-3704.

15.   Savoldo B, Huls MH, Liu Z, et al. Autologous Epstein-Barr virus (EBV)-specific cytotoxic T cells for the treatment of persistent active EBV infection. *Blood*. 2002;100(12):4059-4066.

16.   Hochberg D, Souza T, Catalina M, Sullivan JL, Luzuriaga K, Thorley-Lawson DA. Acute infection with Epstein-Barr virus targets and overwhelms the peripheral memory B-cell compartment with resting, latently infected cells. *J Virol*. 2004;78(10):5194-5204.

17.   Chaganti S, Heath EM, Bergler W, et al. Epstein-Barr virus colonization of tonsillar and peripheral blood B-cell subsets in primary infection and persistence. *Blood*. 2009;113(25):6372-6381.

18.   Ohga S, Ishimura M, Yoshimoto G, et al. Clonal origin of Epstein-Barr virus (EBV)-infected T/NK-cell subpopulations in EBV-positive T/NK-cell lymphoproliferative disorders of childhood. *J Clin Virol*. 2011;51(1):31-37.

19.   Henter JI, Samuelsson-Horne A, Arico M, et al. Treatment of hemophagocytic lymphohistiocytosis with HLH-94 immunochemotherapy and bone marrow transplantation. *Blood*. 2002;100(7):2367-2373.

20.   Fox CP, Shannon-Lowe C, Gothard P, et al. Epstein-Barr virus-associated hemophagocytic lymphohistiocytosis in adults characterized by high viral genome load within circulating natural killer cells. *Clin Infect Dis*. 2010;51(1):66-69.

21.   Heath E, Begue-Pastor N, Chaganti S, et al. Epstein-Barr virus infection of naive B cells in vitro frequently selects clones with mutated immunoglobulin genotypes: implications for virus biology. *PLoS Pathog*. 2012;8(5):e1002697.

22.   Chen S, Akbar SM, Abe M, Hiasa Y, Onji M. Immunosuppressive functions of hepatic myeloid-derived suppressor cells of normal mice and in a murine model of chronic hepatitis B virus. *Clin Exp Immunol*. 2011;166(1):134-142.

23.   Tacke RS, Lee HC, Goh C, et al. Myeloid suppressor cells induced by hepatitis C virus suppress T-cell responses through the production of reactive oxygen species. *Hepatology*. 2012;55(2):343-353.

24.   Vollbrecht T, Stirner R, Tufman A, et al. Chronic progressive HIV-1 infection is associated with elevated levels of myeloid-derived suppressor cells. *AIDS*. 2012;26(12):F31-37.

25.   Gabrilovich DI, Nagaraj S. Myeloid-derived suppressor cells as regulators of the immune system. *Nat Rev Immunol*. 2009;9(3):162-174.

26.   Veglia F, Perego M, Gabrilovich D. Myeloid-derived suppressor cells coming of age. *Nat Immunol*. 2018;19(2):108-119.

27.   Dorhoi A, Glaria E, Garcia-Tellez T, et al. MDSCs in infectious diseases: regulation, roles, and readjustment. *Cancer Immunol Immunother*. 2019;68(4):673-685.

28.   Condamine T, Gabrilovich DI. Molecular mechanisms regulating myeloid-derived suppressor cell differentiation and function. *Trends Immunol*. 2011;32(1):19-25.

TABLES

Table 1. Antibodies used in flow cytometry and FlowRNA

	Antibody	**Fluorophore**	**Clone**	**Company**
Cell surface	CD3	AF700	OKT3	eBioscience
	CD3	APC	SK7	BD
	CD4	ECD	T4	Beckman Coulter
	CD8	AF488	HIT8a	Biolegend
	CD8	BV650	SK1	Biolegend
	CD11b	FITC	ICRF44	Biolegend
	CD14	Pacific blue	M5E2	Biolegend
	CD15	PE/Dazzle 594	SSEA-1	Biolegend
	CD16	BV650	3G8	Biolegend
	CD20	AF700	2h7	Biolegend
	CD25	PE	M-A251	Biolegend
	CD33	PE	P67.6	Biolegend
	CD38	PE-Cy7	HB-7	Biolegend
	CD45RA	BV711	HI100	Biolegend
	CD56	PE	MEM0188	ThermoFisher
	CD56	ECD	N901	Beckman Coulter
	CD197 (CCR7)	PE	G043H7	Biolegend
	HLA-DR/DP/DQ	PE-Cy7	Tu39	Biolegend
	TCRγ/δ	PE	B1	Biolegend
Intracellular	FoxP3	PE-Cy7	PCH101	eBioscience
	Eomes	PE	WD1928	eBioscience
	Perforin	PE-Cy7	dG9	BD
	Ki67	BV786	B56	BD
	Granzyme B	AF700	GB11	BD

Table 2. Clinical characteristics of patients with EBV-associated LPDs

Pt	Age/ gender	History	Presentation	Diagnosis	EBV PCR (copies/ml)	Treatment	Outcome
1	46/M	Chronic plantar warts	Lonstanding constitutional symptoms	CAEBV	3.8×10^5	None	Alive, lost to follow-up
2	19/M	Crohn's on IS therapy (6-mercaptopurine)	Acute illness with clinical and laboratory features of HLH	HLH secondary to EBV infection	1.54×10^5	Rituximab, steroids and etoposide	Alive.
3	21/M	Fevers, night sweats, weight loss	Acute illness with clinical and laboratory features of HLH.	HLH with CAEBV	3×10^6	R-CHOP Etoposide and corticosteroids. FMT conditioning then HSCT	Recurrence of disease and death
4	54/M		Sub-acute illness with weight loss and gastrointestinal symptoms	CAEBV, gastric involvement	1.4×10^6	Steroids then gemcitabine, dexamethasone and cisplatin	Death with PD and visceral perforation
5	27/M	Ulcerative colitis, on infliximab	Rapid deterioration with fevers, cytopenias and hepatosplenomegaly	ANKL	1.99×10^6	Corticosteroids	Death

HLH, haemophagocytic lymphohistiocytosis: CAEBV, Chronic Active EBV; ANKL, Aggressive NK leukaemia; R-CHOP, Rituximab, Cyclophosphamide, Doxorubicin, Vincristine, Prednisolone; FMT, Fludarabine, Melphalan, Thiotepa; HSCT, human stem cell transplant.

FIGURE LEGENDS

FIGURE 1. **Multicolour FlowRNA protocol to identify the phenotype and function of the EBV-infected lymphocytes.** (a) Mononuclear cells were isolated from peripheral blood, stained for lymphocyte lineage markers then fixed and permeabilised. Intracellular markers were then stained and the cells subject to fluorescence in situ hybridisation (FlowRNA) for the virally encoded EBERs and housekeeping cellular B2M. (b) EBV+/GFP+ Akata cells were added to EBV-/GFP- Akata cells at decreasing percentages (100%, 3%, 1%) and examined by FlowRNA to determine the sensitivity and specificity of the assay. (c) Lymphocytes were identified by forward vs side scatter and single cells were gated, dead and myeloid cells were excluded from further analysis. (d) The stained cells were examined by flow cytometry and plotted as CD19, CD3, CD4, CD8 and CD56 vs EBER to determine the subset of cells infected with EBV (dual positive). The upper panel shows a representative assay performed on blood of a healthy EBV carrier where no EBV-infected cells were detected. The lower panel shows a representative assay performed on the blood of a T/NK LPD patient and clearly shows CD3+, CD8+ and CD19+ lymphocyte populations expressing EBERs. The percentage of total CD19+ B-cells and total CD3+, CD8+ T-cells is given in the upper right hand quadrant.

FIGURE 2. Identification of EBV-infected lymphocytes and clonality in the peripheral blood of patients. (a) Multicolour FlowRNA cytometric analysis of PBMCs from patients 1 and 2 revealed EBV infection of CD19+ B-cells. (b) FlowRNA analysis of PBMC from patients 3, 4 and 5 revealed EBV infection of CD4+ T-cells from patient 3 and 4, and EBV infection of CD56^{high} NK-cells, CD4+ and CD8+ T-cells. The analysis also revealed downregulation of CD3 expression in the EBER^{POS} across patients 3 to 5. The percentage of total lymphocyte subsets expressing EBERs is given in the upper right hand quadrant. (c) T-cells were stained with a panel of 24 antibodies against the TCR-BV epitopes and analysed by flow cytometry. The % of T-cells expressing each TCR-BV are represented by Venn diagrams. For patients 3, 4 and 5, all EBER^{NEG} T-cells exhibited polyclonal TCR-BV populations. However, the EBER^{POS} CD4+ T-cells from patients 3 and 4 exhibited a large monoclonal TCR-BV expansion (TCR-BV8 for patient 3 and TCR-BV12 for patient 4). In contrast, EBER^{POS} CD4+ T-cells from patient 5 exhibited a polyclonal TCR-BV population whereas the CD8+ T-cell exhibited a more focussed TCR-BV population (TCR-BV13.2). Key: TCR-BV usage.

FIGURE 3. **EBER^{POS} and EBER^{NEG} cells exhibit differences in their phenotype and function.** (a) EBER^{POS} and EBER^{NEG} CD4+ T-cells from patients 3 and 4 were stained for CCR7 and CD45RA (top row), Ki-67 and CD38 (second row), Foxp3 and CD25 (third row) and TNFα and IFNγ (bottom row). Age-matched healthy donors were also analysed; two representative donors are shown. The analysis revealed the EBER^{POS} cell expressed markers consistent with memory T-cells, they were activated and proliferative, they were not Tregs and they expressed significant amounts of pro-inflammatory cytoines. In contrast, The EBER^{NEG} CD4+ T-cells closely resembled the phenotype and function of the healthy donor CD4+ T-cells.

FIGURE 4. **EBV-infected CD4+ T-cells are resistant to conventional treatment regimens for CAEBV and HLH.** (a) FlowRNA was performed on patient PBMCs to monitor outcome following treatment; both pre- and post-treatment samples are shown for patients 3

21

and 4. The percentage of EBER^{POS} CD4+ T-cells is shown in the upper right quadrant. The analyses revealed an increase in the number of EBV-infected CD4+ T-cells following treatment. (b) FlowRNA performed on PBMCs from patient 3, one month before HSCT (- 1 month) and 16 months post-HSCT and shows a sustained loss of EBER^{POS} lymphocytes. However, analysis at 23 months post-HSCT revealed a significant population of EBER^{POS} CD4+ T-cells. The percentage of EBER^{POS} CD4+ T-cells is shown in the upper right quadrant. (c) Analysis of the EBER^{POS} CD4+ T-cells identified at 23 months revealed the reappearance of the EBV-infected TCR-BV8 clone originally identified in the first sample.

FIGURE 5. **Phenotype and function of EBER^{POS} T and NK-cells from patient 5.**
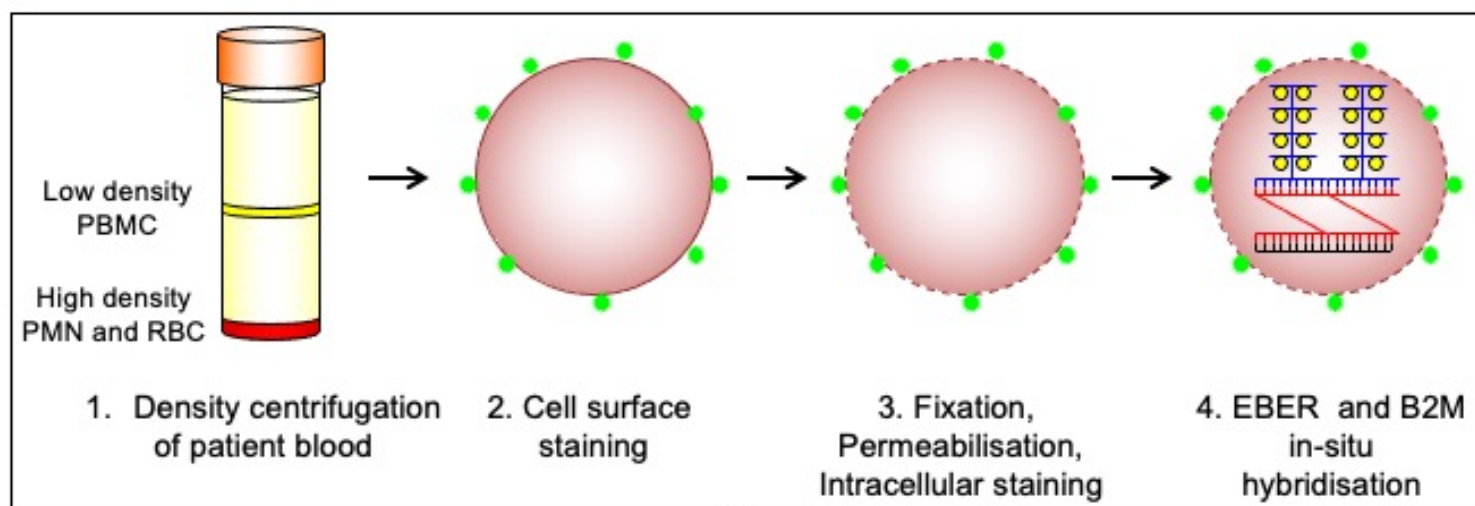FlowRNA analysis of EBER^{POS} and EBER^{NEG} CD4+ and CD8+ T-cells from patient 5. PBMC were stained for CCR7 and CD45RA (top row), Ki-67 and CD38 (second row), Foxp3 and CD25 (third row) and TNFα and IFNγ (bottom row). Age-matched healthy donors were also analysed; one representative donor is shown. The phenotype and function of the EBER^{POS} CD4+ T-cells closely resembled that of the EBER^{NEG} CD4+ T-cells and the healthy donors. The EBER^{POS} CD8+ T-cells were more activated and all expressed IFNγ and TNFα. (c) Total NK-cells from patient 5 were stained for CD45RA and CCR7 (top row), Ki-67 and CD38 (second row) and TNFα and IFNγ (bottom row). Analysis of NK-cells from one representative healthy donor is shown. All the EBER^{POS} NK-cells were highly activated and replicative, and they all expressed IFNγ.

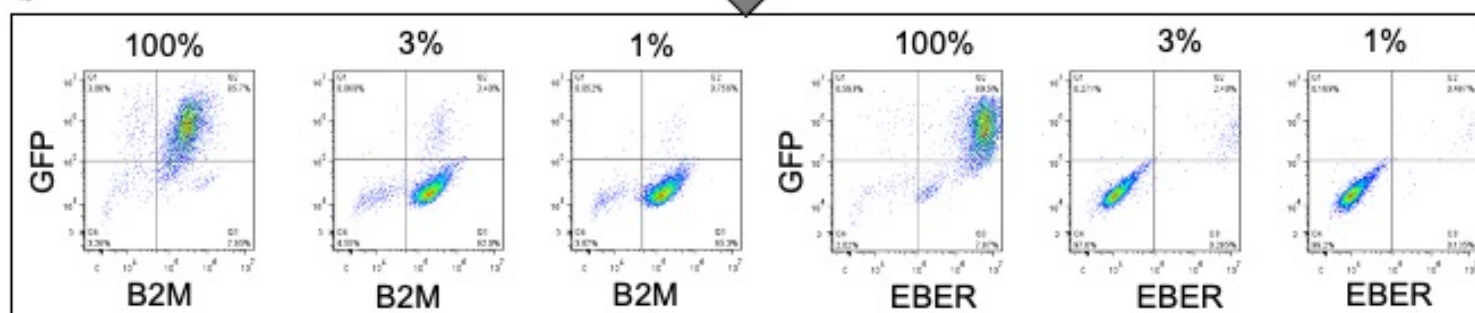**FIGURE 6**. **Granulocytic myeloid-derived suppressor cells are expanded in the blood of patients and potently inhibit T-cell responses.** (a) Flow cytometric analysis of fresh patient PBMC by FSC vs SSC showed the presence of large granular cells (G-MDSCs), shown in blue; % of G-MDSCs to total PBMCs isolated is shown. A representative healthy donor is shown for comparison. (b) The % of G-MDSC is plotted with the mean compared to the mean from 10 healthy donors. A two-tailed Mann-Whitney test was used to compare groups. (c) Nuclear morphology of G-MDSCs (low density) and neutrophils (high density) revealed characteristic band cell/neutrophil morphology by H&E staining. (d) Flow cytometric analysis of the G-MDSC revealed expression of CD11b, CD15, CD16, CD33 but no expression of HLA II. Isotype controls (grey filled histogram) are shown. (e) Luminex assays for GM-CSF, IL-1β, IL-6 and TNFα were performed upon patient plasma and compared to healthy donors. All patients had higher concentrations of these cytokines in their plasma than the healthy donors. Dashed horizontal line indicates the limit of accurate detection. (f) Luminex assay was used to determine the concentration of arginase-1 in the plasma of CAEBV and EBV-HLH patients, and healthy donors. Dashed horizontal line indicates the limit of accurate detection. (g) Inhibition of T-cell proliferation by MDSCs was measured following co-culture of T-cells with decreasing numbers of G-MDSCs (T:G-MDSC range 1:1 to 1:0.125). The percentage T-cell proliferation in the presence of G-MDSCs is plotted relative to T-cells alone. Data shown is an average of 3 patients. (h) The inhibition of T-cell proliferation by G-MDSCs from patients and healthy donors at a T-cell:G-MDSC ratio of 1:1 is plotted. Proliferation is shown relative to control (T-cells stimulated in the absence of MDSCs). In (g) and (h), a Kruskall-Wallis test was used to compare groups. In (b), (e) and (f), each patient is represented by a unique symbol as follows; patient 1 = +, patient 2 = x, patient 3 = o, patient 4 = Δ and patient 5 = □.
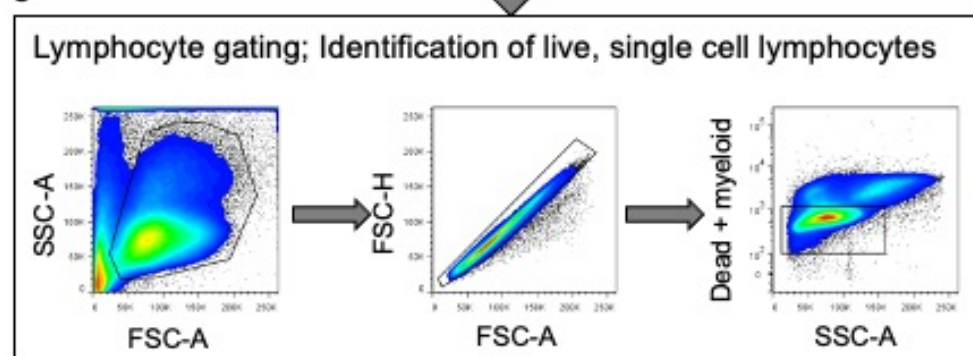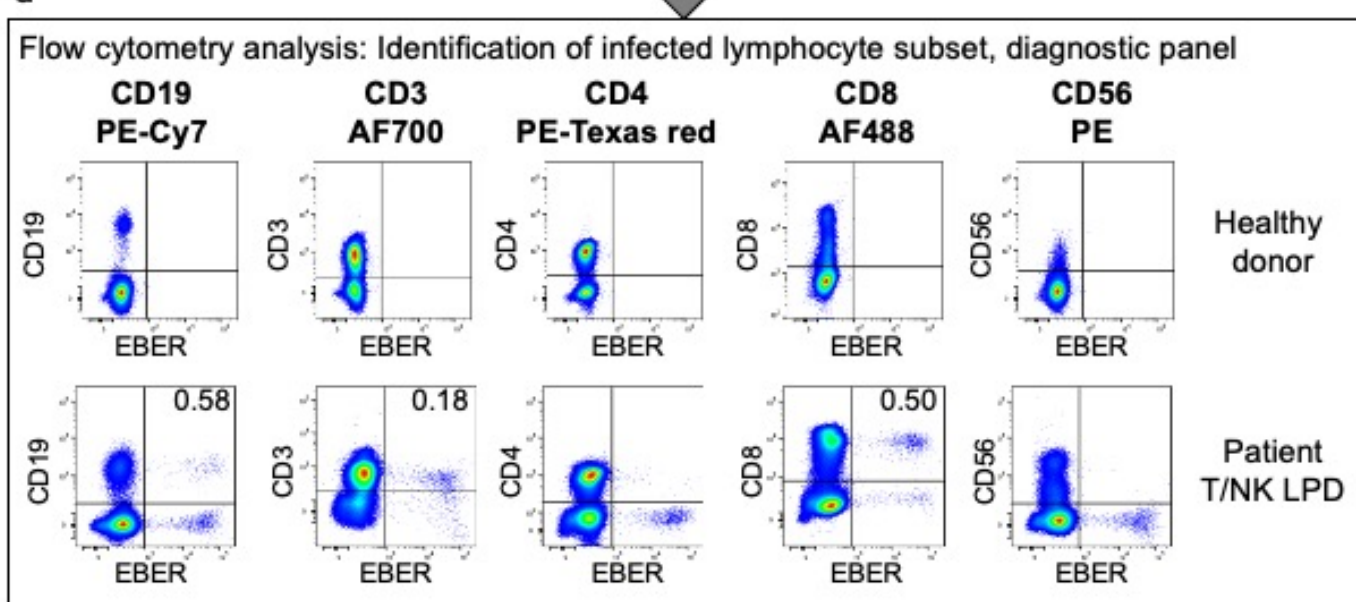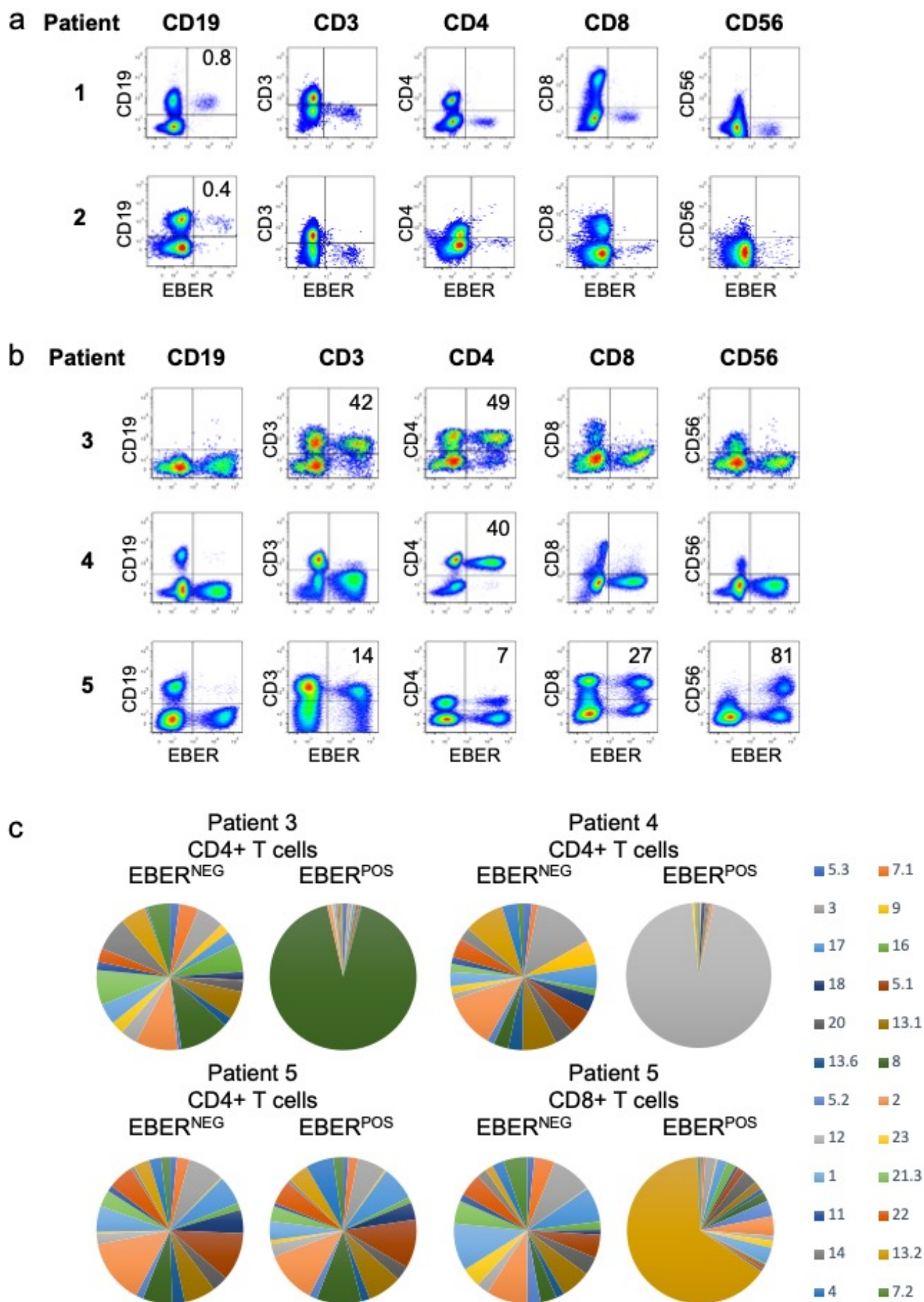
Figure 1.

a

1. Density centrifugation of patient blood
2. Cell surface staining
3. Fixation, Permeabilisation, Intracellular staining
4. EBER and B2M in-situ hybridisation

Low density PBMC

High density PMN and RBC

b

100%   3%   1%   100%   3%   1%

GFP — B2M   B2M   B2M   EBER   EBER   EBER

c

Lymphocyte gating; Identification of live, single cell lymphocytes

SSC-A / FSC-A   →   FSC-H / FSC-A   →   Dead + myeloid / SSC-A

d

Flow cytometry analysis: Identification of infected lymphocyte subset, diagnostic panel

| CD19 PE-Cy7 | CD3 AF700 | CD4 PE-Texas red | CD8 AF488 | CD56 PE | |

Healthy donor

Patient T/NK LPD

0.58   0.18   0.50

Figure 2

Figure 3

Healthy donor: CD4+ cells
Donor 1   Donor 2
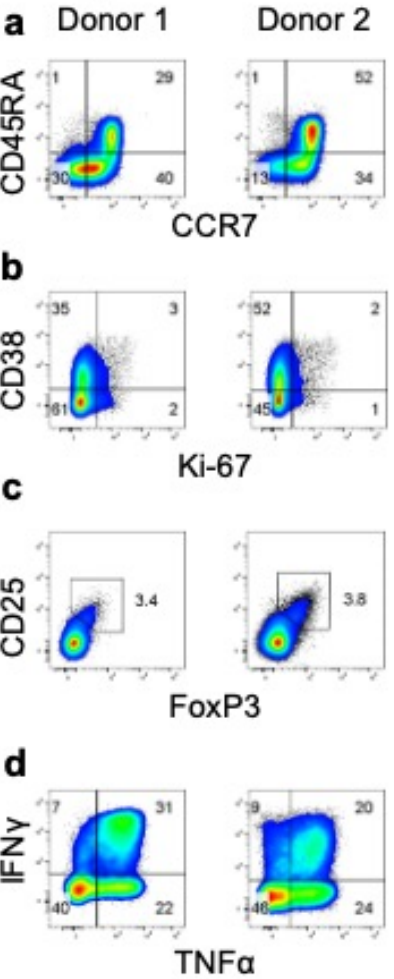
Patient 3: CD4+ cells
EBERneg   EBERpos
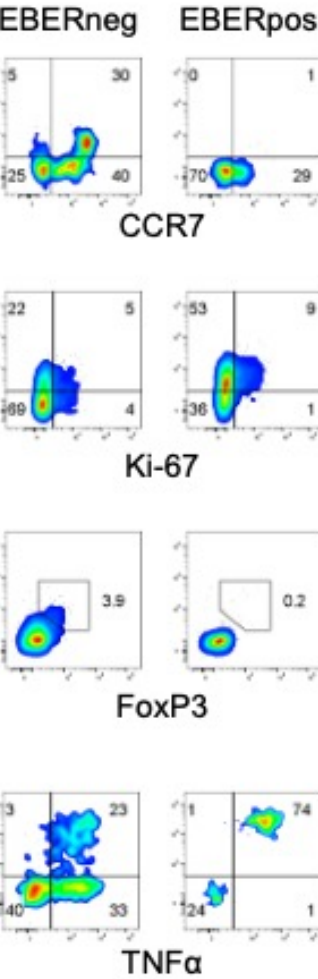
Patient 4: CD4+ cells
EBERneg   EBERpos

Figure 4

Figure 5

Figure 6